

Nonlinear elastic effects in group III-Nitrides: From *ab initio* to finite element calculation

Michal Petrov¹, Liverios Lymperakis¹, Jörg Neugebauer¹, Robert Stefaniuk² and Paweł Dłużewski²

¹ Max-Planck-Institut für Eisenforschung, Max-Planck-Strasse 1, Düsseldorf, Germany

² Institute of Fundamental Technological Research PAS, Świętokrzyska 21, 00-049 Warsaw, Poland.
e-mail: petrov@mpie.de

Abstract

III-Nitride based nanostructures, such as Quantum Dots (QDs), are of great interest due to their potential optoelectronic applications. In this work we combine *ab-initio* calculations and Finite Element Method (FEM) calculations in a multi-scheme approach and we investigate the properties of a GaN QD embedded in AlN barrier. Based on first principles calculations we derive the second and third order elastic constants for AlGaIn alloys within the framework of anisotropic hyperelasticity [3]. The dependence of the elastic constants on the alloy composition as well as on the strain measure is explored. In a second step the aforementioned elastic constants are used as input for FEM calculations of the electro-mechanically coupled non-linear boundary problem of the strain and polarization constitutive equations. We find that the electric field along the growth direction varies significantly, an effect which has interesting implications on the spatial localization of the carriers. Although our calculations reveal that qualitatively the electric potential distribution does not depend sensitively on the third order elastic constants, it was found that the inclusion of the non-linear effects in our FEM calculations may quantitatively affect it by more than 5%.

Keywords: *ab initio, finite element method, elastic constants, III-Nitrides*

1. Introduction

The group III-Nitride semiconductors (AlN, GaN, and InN) are by now well established as a key material system for optoelectronic applications. The reason for the big interest in these materials is manifold: They have direct bandgaps in the range between 0.7-6.2 eV (from 0.7-0.8 eV for InN - see [2], [11] and Refs therein - and 3.4 eV for GaN to 6.2 eV for AlN [1]) which covers the entire visible and extends into the ultraviolet (UV) region of the optical spectrum. Because of their wide bandgap and strong bond strength, this materials system is suitable for violet, blue, and green light emitting devices (e.g., for full color displays, laser printers, high density information storage, or under water communication) and for high-temperature/high-power transistors (as needed e.g., in automobile engines, power distribution systems, or to design all electric vehicles). Another important property of III-Nitrides is that they can be alloyed, and thus they enable bandgap engineering and subsequently tuning of the emission wavelengths. On the other hand semiconductor based nanostructures, like Quantum Dots (QDs), are of great interest both from the fundamental point of view as well as for their potential optoelectronic applications: The zero-dimensional nature of Quantum Dots (QD) provides a more efficient carrier localization and results in superior characteristics with respect to their optical properties.

In this work we combine *ab-initio* with Finite Elements Method (FEM) calculations in order to study the strain, electric, and polarization fields in a system of a GaN QD embedded in AlN matrix. In group III-nitrides, due to the large lattice mismatch and the stiffness of the material, the quantum dots embedded in the semiconductor matrix are highly strained and the inclusion of nonlinear elastic effects is crucial. However, so far experimental and/or theoretical data on the composition and stress dependence of the elastic constants of AlGaIn alloys are still lacking. Thus, in a first step we perform first principles calculations in order to derive the second and third order elastic constants of AlGaIn alloys. In a second step these constants are used as in-

put for FEM calculations: we solve the constitutive equations for the stress and polarization field. In most of the previous numerical simulations, the converse piezoelectric effect was neglected in FE analysis of nitrides, cf. [9]. Such simplified approach is based on solving separately two boundary-value problems: First the problem $\text{div } \boldsymbol{\sigma} = \mathbf{0}$ is solved, and next the problem $\text{div } \mathbf{P} = 0$ for fixed $\boldsymbol{\varepsilon}(\mathbf{x})$. Contrary to that, in this work we solve a single boundary-value problem stated for full electro-mechanical coupling in which the final strain field results from the mechanical stress equilibrium and converse piezoelectric effect. Based on these calculations we derive the strain and electric field associated with the GaN/AlN QD.

The paper is organized as follows. First the definition of the strain measures and the second and third order elastic constants associated with the wurtzitic symmetry are given in Sections 2 and 3 respectively. Next a detailed description of the *ab-initio* calculations on the third order elastic constants is given and their dependence on the strain measure is discussed. In Sections 5 and 6 we focus on the FEM calculations: the strain and electric potential distributions are given and the influence of the non-linearity on the properties of QDs is discussed. Finally in Section 7 we summarize our results.

2. Finite strain measures

In the theory of nonlinear elasticity the deformation tensor \mathbf{F} is decomposed into the (orthogonal) rotation tensor \mathbf{R} and the (symmetric) right or left stretch tensors \mathbf{U} or \mathbf{V} ,

$$\mathbf{F} = \mathbf{R}\mathbf{U} = \mathbf{V}\mathbf{R}. \quad (1)$$

Definition By Lagrangian and Eulerian strain tensors we mean two tensor functions

$$\hat{\boldsymbol{\varepsilon}} \stackrel{\text{df}}{=} f(u_i) \mathbf{u}_i \otimes \mathbf{u}_i \quad \text{and} \quad \boldsymbol{\varepsilon} \stackrel{\text{df}}{=} f(V_i) \mathbf{v}_i \otimes \mathbf{v}_i, \quad (2)$$

where $u_i, \mathbf{u}_i, V_i, \mathbf{v}_i$ denote respectively the i -th eigenvalues and unit eigenvectors of the right and left stretch tensors, while $f(\cdot)$

denotes an arbitrarily chosen C^1 monotonically increasing function $f(x) : R^+ \ni x \rightarrow f \in R$ which satisfies the conditions $f(x)|_{x=1} = 0$ and $\frac{df(x)}{dx}|_{x=1} = 1$.

This definition includes the well-known Seth-Hill family of the Lagrangian and Eulerian strain measures:

$$\widehat{\boldsymbol{\varepsilon}} \stackrel{df}{=} \begin{cases} \frac{1}{m}(\mathbf{U}^m - \mathbf{1}) & \text{for } m \neq 0, \\ \ln \mathbf{U} & \text{for } m = 0, \end{cases} \quad (3)$$

and

$$\boldsymbol{\varepsilon} \stackrel{df}{=} \begin{cases} \frac{1}{m}(\mathbf{V}^m - \mathbf{1}) & \text{for } m \neq 0, \\ \ln \mathbf{V} & \text{for } m = 0, \end{cases} \quad (4)$$

where m is a real number. This family, called often a family of generalized strain measures, was noted first by Seth [12] and next it has been widely popularized thanks to papers by Hill [7]. Our definition includes not only strains from the Seth-Hill family but also many others, cf. [4].

3. Second and third order elastic constants

The third-order elastic constants are determinable experimentally by measurement of small changes of ultrasonic wave velocities in stressed crystals. Contrary to the traditional (second-order) elastic constants the third order elastic constants depend sensitively on the strain measure. Usually, the constants are determined for the Green strain measure which corresponds to the Lagrangian strain (see Eqn 3) for $m = 2$ and it is often called the Lagrangian strain (see for example Refs [3, 14, 6, 16]).

In order to demonstrate the sensitive dependence of the constants on the choice of the strain measure, let us first assume that a hyperelastic material satisfies the following specific strain energy function:

$$\psi(\widehat{\boldsymbol{\varepsilon}}) = \frac{1}{\widehat{\rho}} \left[\frac{1}{2!} \widehat{C}^{ijkl} \widehat{\varepsilon}_{ij} \widehat{\varepsilon}_{kl} + \frac{1}{3!} \widehat{C}^{ijklmn} \widehat{\varepsilon}_{ij} \widehat{\varepsilon}_{kl} \widehat{\varepsilon}_{mn} \right], \quad (5)$$

where $\widehat{\mathbf{c}}$ and $\widehat{\mathbf{C}}$ are tensors of the second- and third-order elastic constants, and $\widehat{\rho}$ denotes the mass density corresponding to the volume of undeformed lattice. In other words ψ is the specific energy corresponding not to the volume but to the mass of crystal. Differentiation of the last equation over general strain gives the following equation for the conjugate stress:

$$\widehat{\boldsymbol{\sigma}} = \widehat{\mathbf{c}} : \widehat{\boldsymbol{\varepsilon}} + \frac{1}{2} \widehat{\boldsymbol{\varepsilon}} : \widehat{\mathbf{C}} : \widehat{\boldsymbol{\varepsilon}}, \quad (6)$$

where the colon denotes the double scalar product over two sequential indices. Usually, the third-order elastic constants are determined in relation to the Green strain measure, i.e. $\widehat{\boldsymbol{\varepsilon}} = \frac{1}{2}(\mathbf{U}^2 - \mathbf{1})$. Obviously, we can rewrite (5) by using another strain measure. Let us assume for example $m' = 0$, i.e. $\widehat{\boldsymbol{\varepsilon}}' = \ln \mathbf{U}$. By solving the last relation with respect to \mathbf{U} and substituting into (3) we find the following relation between the respective eigenvalues of $\widehat{\boldsymbol{\varepsilon}}$ and $\widehat{\boldsymbol{\varepsilon}}'$:

$$\widehat{\varepsilon}_i(\widehat{\boldsymbol{\varepsilon}}') = \begin{cases} \frac{1}{m} \left[(m' \widehat{\varepsilon}'_i + 1)^{\frac{m}{m'}} - 1 \right] & \text{for } m \neq 0, m' \neq 0, \\ \frac{1}{m} (e^{m \widehat{\varepsilon}'_i} - 1) & \text{for } m \neq 0, m' = 0, \\ \frac{1}{m'} \ln (m' \widehat{\varepsilon}'_i + 1) & \text{for } m = 0, m' \neq 0, \end{cases} \quad (7)$$

where $\widehat{\varepsilon}'_i$ is the i^{th} eigenvalue of $\widehat{\boldsymbol{\varepsilon}}'$ while \mathbf{u}_i is the eigenvector both of $\widehat{\boldsymbol{\varepsilon}}'$, $\widehat{\boldsymbol{\varepsilon}}$ and \mathbf{U} . Let us decompose the specific internal energy function into a power series

$$\psi(\widehat{\boldsymbol{\varepsilon}}(\widehat{\boldsymbol{\varepsilon}}')) = \frac{1}{\widehat{\rho}} \left[\frac{1}{2!} \widehat{C}'^{ijkl} \widehat{\varepsilon}'_{ij} \widehat{\varepsilon}'_{kl} + \frac{1}{3!} \widehat{C}'^{ijklmn} \widehat{\varepsilon}'_{ij} \widehat{\varepsilon}'_{kl} \widehat{\varepsilon}'_{mn} + \dots \right], \quad (8)$$

where:

$$\mathbf{c}' = \frac{1}{\widehat{\rho} 2!} \left. \frac{\partial^2 \psi(\widehat{\boldsymbol{\varepsilon}}(\widehat{\boldsymbol{\varepsilon}}'))}{\partial \widehat{\boldsymbol{\varepsilon}}' \partial \widehat{\boldsymbol{\varepsilon}}'} \right|_{\widehat{\boldsymbol{\varepsilon}}' = \mathbf{0}}, \quad (9)$$

$$\mathbf{C}' = \frac{1}{\widehat{\rho} 3!} \left. \frac{\partial^3 \psi(\widehat{\boldsymbol{\varepsilon}}(\widehat{\boldsymbol{\varepsilon}}'))}{\partial \widehat{\boldsymbol{\varepsilon}}' \partial \widehat{\boldsymbol{\varepsilon}}' \partial \widehat{\boldsymbol{\varepsilon}}'} \right|_{\widehat{\boldsymbol{\varepsilon}}' = \mathbf{0}}. \quad (10)$$

Substitution of (8) and (7) into (10) followed by use of the known formula for derivatives of an isotropic proper-symmetric fourth-order tensor function of a symmetric second-order tensor we find:

$$\widehat{C}'^{ijkl} = \widehat{c}^{ijkl}, \quad (11)$$

$$\widehat{C}'^{ijklmn} = \widehat{C}^{ijklmn} + (m - m') [\mathcal{J}^{ijkl} {}_{ab} \widehat{c}^{abmn} + \mathcal{J}^{klmn} {}_{ab} \widehat{c}^{abij} + \mathcal{J}^{mnij} {}_{ab} \widehat{c}^{abkl}], \quad (12)$$

where the representation of \mathcal{J} written in any chosen orthonormal coordinate set takes the form [5]:

$$\mathcal{J}_{ijklmn} = \frac{1}{8} (\delta_{ik} \delta_{jm} \delta_{ln} + \delta_{ik} \delta_{jn} \delta_{lm} + \delta_{il} \delta_{jm} \delta_{kn} + \delta_{il} \delta_{jn} \delta_{km} + \delta_{im} \delta_{jk} \delta_{ln} + \delta_{im} \delta_{jl} \delta_{kn} + \delta_{in} \delta_{jk} \delta_{lm} + \delta_{in} \delta_{jl} \delta_{km}). \quad (13)$$

3.1. Elastic constants for hexagonal crystals

Since the strain and stress tensors are symmetric, only six among nine stress/strain components are independent. Therefore it is convenient to use the Voight notation reducing the number of subscripts $11 \rightarrow 1, 22 \rightarrow 2, 33 \rightarrow 3, 23 \rightarrow 4, 13 \rightarrow 5, 12 \rightarrow 6$. Then we can rewrite (6) in the form:

$$\widehat{\sigma}_i = \widehat{c}_{ij} \widehat{\varepsilon}_j + \frac{1}{2} \widehat{C}_{ijk} \widehat{\varepsilon}_j \widehat{\varepsilon}_k, \quad (14)$$

It is worth emphasizing that in the Voight notation the mixed components of strains are double while the analogical stress components are single. Therefore in some cases another notation based on the so-called normalized measures, where the shear stress and strain components are multiplied by $\sqrt{2}$, are used. Nevertheless, the normalized stress/strain notations seem to be inconvenient in the case of the use of third order elastic constants.

3.2. Hexagonal systems

The following point symmetry groups are included to hexagonal symmetry: $6, \bar{6}, \frac{6}{m}, 622, 6mm, \bar{6}m2, \frac{6}{m}mm$. From the viewpoint of symmetry of the elastic constants the group can be divided into two subsystems, called respectively subsystems 10 and 11. Nevertheless, for the second order elastic tensor the mentioned subsystems makes no difference. The difference between the subsystems manifests only the higher order constants, e.g. the third order constants.

For hexagonal systems the representation of the second order elastic tensor is composed of five mutually independent elastic constants, $\widehat{c}_{11}, \widehat{c}_{12}, \widehat{c}_{13}, \widehat{c}_{33}$ and \widehat{c}_{44} :

$$[\widehat{c}_{ij}] = \begin{bmatrix} \widehat{c}_{11} & \widehat{c}_{12} & \widehat{c}_{13} & \cdot & \cdot & \cdot \\ \widehat{c}_{12} & \widehat{c}_{11} & \widehat{c}_{13} & \cdot & \cdot & \cdot \\ \widehat{c}_{13} & \widehat{c}_{13} & \widehat{c}_{33} & \cdot & \cdot & \cdot \\ \cdot & \cdot & \cdot & \widehat{c}_{44} & \cdot & \cdot \\ \cdot & \cdot & \cdot & \cdot & \widehat{c}_{44} & \cdot \\ \cdot & \cdot & \cdot & \cdot & \cdot & \frac{1}{2}(\widehat{c}_{11} - \widehat{c}_{12}) \end{bmatrix}. \quad (15)$$

For hexagonal systems we find two two-fold eigenvalues, $\widehat{c}_1, \widehat{c}_3$ and two one-fold eigenvalues $\widehat{c}_2, \widehat{c}_4$ which correspond to the following eigenvectors, cf. [13]:

$$\begin{aligned} [\widehat{\boldsymbol{\varepsilon}}_{1/2}] &= \begin{bmatrix} 1 \\ \cdot \\ \cdot \\ \cdot \\ \cdot \\ \cdot \end{bmatrix} + k_{1/2} \begin{bmatrix} \cdot \\ \cdot \\ \cdot \\ \cdot \\ \cdot \\ \cdot \end{bmatrix}, & [\widehat{\boldsymbol{\varepsilon}}_2] &= \begin{bmatrix} -1 \\ \cdot \\ \cdot \\ \cdot \\ \cdot \\ \cdot \end{bmatrix}, \\ [\widehat{\boldsymbol{\varepsilon}}_{31}] &= \begin{bmatrix} \cdot \\ \cdot \\ 1 \\ \cdot \\ \cdot \\ \cdot \end{bmatrix}, & [\widehat{\boldsymbol{\varepsilon}}_{32}] &= \begin{bmatrix} \cdot \\ \cdot \\ \cdot \\ \cdot \\ 1 \\ \cdot \end{bmatrix}, & [\widehat{\boldsymbol{\varepsilon}}_4] &= \begin{bmatrix} 1 \\ \cdot \\ \cdot \\ \cdot \\ \cdot \\ \cdot \end{bmatrix}, \end{aligned} \quad (16)$$

where $k_{1/2} = \frac{\widehat{c}_{33} - \widehat{c}_{11} - \widehat{c}_{12} \pm \sqrt{(\widehat{c}_{33} - \widehat{c}_{11} - \widehat{c}_{12})^2 + 8\widehat{c}_{13}^2}}{2\widehat{c}_{13}}$.

The eigenvectors $\widehat{\mathbf{e}}_{11}, \widehat{\mathbf{e}}_{12}$ and $\widehat{\mathbf{e}}_{31}, \widehat{\mathbf{e}}_{32}$ compose respectively the vector bases for two two-dimensional subspaces of eigenvectors. Each linear combination of $\widehat{\mathbf{e}}_{11}$ and $\widehat{\mathbf{e}}_{12}$ gives a vector which is a member of the same subspace. Nevertheless, the elemental vectors from which the eigenvectors $\widehat{\mathbf{e}}_{11/2}$ are built up in (19), i.e. the 6-dimensional vectors $\begin{bmatrix} 1 \\ \cdot \\ \cdot \\ \cdot \\ \cdot \\ \cdot \end{bmatrix}$ and $\begin{bmatrix} \cdot \\ \cdot \\ \cdot \\ \cdot \\ \cdot \\ 1 \end{bmatrix}$, are not members of the mentioned subspace. Only two linear combinations of these two 6th order vectors corresponding to the fixed values k_1 and k_2 span the mentioned subspace.

The subsystem 11 ($\overline{6}m2, 6mm, 622, \frac{6}{m}mm$) of the hexagonal symmetry is the corresponding for wurtzite crystals. In this subsystem we find ten independent third order elastic constants. All non-zero constants are the following: $\widehat{C}_{111}, \widehat{C}_{222}, \widehat{C}_{333}, \widehat{C}_{112}, \widehat{C}_{113}, \widehat{C}_{123}, \widehat{C}_{133}, \widehat{C}_{144}, \widehat{C}_{155}, \widehat{C}_{344}$. As has already been mentioned the third order elastic constants depend sensitively on the strain measure used to determine them. Therefore, changing the strain measure the third order elastic constants must be recalculated according to [5]. For subsystem 11 we find the following transformation rules:

$$\begin{aligned} \widehat{C}'_{111} &= \widehat{C}_{111} + 3(m - m')\widehat{c}_{11}, \\ \widehat{C}'_{144} &= \widehat{C}_{144} + \frac{1}{4}(m - m')(\widehat{c}_{13} + \widehat{c}_{12}), \\ \widehat{C}'_{222} &= \widehat{C}_{222} + 3(m - m')\widehat{c}_{11}, \\ \widehat{C}'_{155} &= \widehat{C}_{155} + \frac{1}{4}(m - m')(\widehat{c}_{13} + \widehat{c}_{11} + 4\widehat{c}_{44}), \\ \widehat{C}'_{333} &= \widehat{C}_{333} + 3(m - m')\widehat{c}_{33}, \\ \widehat{C}'_{344} &= \widehat{C}_{344} + \frac{1}{4}(m - m')(\widehat{c}_{23} + \widehat{c}_{33} + 4\widehat{c}_{44}), \\ \widehat{C}'_{112} &= \widehat{C}_{112} + (m - m')\widehat{c}_{12}, \\ \widehat{C}'_{133} &= \widehat{C}_{133} + (m - m')\widehat{c}_{13}, \\ \widehat{C}'_{113} &= \widehat{C}_{113} + (m - m')\widehat{c}_{13}, \\ \widehat{C}'_{123} &= \widehat{C}_{123}. \end{aligned} \quad (17)$$

In this work the determination of the third order elastic constants is based in the Biot strain measure ($m = 1$):

$$\widehat{\mathbf{e}} = \mathbf{U} - \mathbf{1}. \quad (18)$$

4. *Ab-initio* determination of third order elastic constants.

Previous *ab-initio* calculations on the non-linearity of the elastic constants of group-III Nitrides materials system were performed by a number of volume conserving strain deformations for different pressures/volumes [9]. Although this approach provides the pressure dependence of the elastic constants it cannot be easily extended in order to address the strain measure independent third order elastic constants [5]. In the present work we calculate the 10 independent third order elastic constants of $\text{Al}_x\text{Ga}_{1-x}\text{N}$ alloys using the Biot strain measure [10]. Total energy and force calculations are performed within the Density Functional Theory (DFT) in the plane-wave pseudopotential approach

as implemented in the SFHGX code [8] for six linearly independent strain deformation paths. The Perdew-Berke-Ernzerhof Generalized Gradient Approximation (PBE-GGA) is used to describe exchange and correlation. Soft Troullier-Martin pseudopotentials [15] are used and the Ga 3d electrons are treated in the valence band. The Brillouin zone is sampled by an equivalent $3 \times 3 \times 1$ Monkhorst-Pack k -point sampling for the wurtzite unit cell. The planewaves are expanded up to the value 90 Ry cut-off energy. GaN and AlN have been described within a $1 \times 1 \times 1$ supercell while for the random $\text{Al}_x\text{Ga}_{1-x}\text{N}$ alloys $2 \times 2 \times 2$ supercells have been used. The random alloys were modeled using the Special Quasirandom Structures (SQS) [18].

The 10 independent third order elastic constants for the wurtzite structure are determined by using the Biot strain measure (see Eqn (18)). The corresponding strain deformations are applied along the following trial strain directions:

$$\begin{aligned} [\widehat{\mathbf{e}}_a] &= \begin{bmatrix} \Delta & \cdot & \cdot \\ \cdot & \cdot & \cdot \\ \cdot & \cdot & \cdot \end{bmatrix}, & [\widehat{\mathbf{e}}_b] &= \begin{bmatrix} \cdot & \Delta & \cdot \\ \cdot & \cdot & \cdot \\ \cdot & \cdot & \cdot \end{bmatrix}, & [\widehat{\mathbf{e}}_c] &= \begin{bmatrix} \cdot & \cdot & \Delta \\ \cdot & \cdot & \cdot \\ \cdot & \cdot & \cdot \end{bmatrix}, \\ [\widehat{\mathbf{e}}_d] &= \begin{bmatrix} \cdot & \cdot & \frac{\Delta}{2} \\ \cdot & \cdot & \cdot \\ \cdot & \cdot & \cdot \end{bmatrix}, & [\widehat{\mathbf{e}}_e] &= \begin{bmatrix} \cdot & \cdot & \frac{\Delta}{2} \\ \cdot & \cdot & \cdot \\ \cdot & \cdot & \cdot \end{bmatrix}, & [\widehat{\mathbf{e}}_f] &= \begin{bmatrix} \cdot & \frac{\Delta}{2} & \cdot \\ \cdot & \cdot & \cdot \\ \cdot & \cdot & \cdot \end{bmatrix}. \end{aligned} \quad (19)$$

The second and third order elastic constant are calculated using the second and third order derivatives¹ of the total energy:

$$\widehat{c}_{ij} = \widehat{\rho} \frac{\partial^2 \psi}{\partial \widehat{\mathbf{e}}_i \partial \widehat{\mathbf{e}}_j}, \quad (20)$$

$$\widehat{C}_{ijk} = \widehat{\rho} \frac{\partial^3 \psi}{\partial \widehat{\mathbf{e}}_i \partial \widehat{\mathbf{e}}_j \partial \widehat{\mathbf{e}}_k}, \quad (21)$$

where the total deformation gradient is obtained as $\mathbf{F} = \mathbf{F}_i \mathbf{F}_j \mathbf{F}_k$ where:

$$\mathbf{F}_i = \mathbf{1} + \widehat{\mathbf{e}}_i. \quad (22)$$

Using the total deformation gradient we can determine the current position of any crystallographic axis, e.g.

$$\mathbf{a}_1 = \mathbf{F} \widehat{\mathbf{a}}_1, \quad \mathbf{a}_2 = \mathbf{F} \widehat{\mathbf{a}}_2, \quad \mathbf{c} = \mathbf{F} \widehat{\mathbf{c}}, \quad (23)$$

where $\mathbf{a}_1, \mathbf{a}_2, \mathbf{c}$ and $\widehat{\mathbf{a}}_1, \widehat{\mathbf{a}}_2, \widehat{\mathbf{c}}$ denote the main crystallographic axes for the current and reference configurations, respectively. The mesh step Δ is as small as 0.005. The calculated second and third order elastic constants for GaN and AlN are listed in Tables 2 and 1 respectively.

Additionally, using Eqn (17) the third order elastic constants obtained for the Biot strain have been recalculated to the Hencky (logarithmic) and Green (also called Lagrangian) strain and gathered together in Table 2. Contrary to the third order elastic constants the second order ones are invariant with respect to the strain measure.

¹The Finite Difference Method gives the following formulas for the second and third order derivatives of strain energy $\frac{\partial^2 \psi_{i,j,k}}{\partial^2 x} = \frac{\psi_{i+1,j,k} - 2\psi_{i,j,k} + \psi_{i-1,j,k}}{\Delta_x^2}$,

$$\frac{\partial^2 \psi_{i,j,k}}{\partial x \partial y} = \frac{\psi_{i+1,j+1,k} - \psi_{i-1,j+1,k} - \psi_{i+1,j-1,k} + \psi_{i-1,j-1,k}}{4\Delta_x \Delta_y},$$

$$\frac{\partial^3 \psi_{i,j,k}}{\partial^3 x} = \frac{\psi_{i+2,j,k} - \psi_{i-2,j,k} - 2\psi_{i+1,j,k} + 2\psi_{i-1,j,k}}{2\Delta_x^3},$$

$$\frac{\partial^3 \psi_{i,j,k}}{\partial x \partial y \partial z} = \frac{\psi_{i+1,j+1,k+1} - \psi_{i-1,j+1,k+1} - \psi_{i+1,j-1,k+1} + \psi_{i-1,j-1,k+1}}{8\Delta_x \Delta_y \Delta_z} + \frac{-\psi_{i+1,j+1,k-1} + \psi_{i-1,j+1,k-1} + \psi_{i+1,j-1,k-1} - \psi_{i-1,j-1,k-1}}{8\Delta_x \Delta_y \Delta_z},$$

$$\frac{\partial^3 \psi_{i,j,k}}{\partial^2 x \partial y} = \frac{\psi_{i+1,j+1,k} - \psi_{i+1,j-1,k} - 2\psi_{i,j+1,k} + 2\psi_{i,j-1,k} + \psi_{i-1,j+1,k} - \psi_{i-1,j-1,k}}{2\Delta_x^2 \Delta_y},$$

where the respective finite differences in 3 among 6 independent sequential strain directions (19) are $\Delta_x = x_{i+1} - x_i$, $\Delta_y = x_{i+1} - x_i$, $\Delta_z = x_{i+1} - x_i$.

Table 1: Second order elastic constants [in GPa] determined by *ab-initio* calculations. Our calculations of the second order elastic constants of random $\text{Al}_x\text{Ga}_{1-x}\text{N}$ alloys for $x=0.25, 0.5,$ and 0.75 (not listed here) reveal an almost linear behavior with respect to alloy composition.

GaN						AlN					
\hat{c}_{11}	\hat{c}_{12}	\hat{c}_{13}	\hat{c}_{33}	\hat{c}_{44}	\hat{c}_{66}	\hat{c}_{11}	\hat{c}_{12}	\hat{c}_{13}	\hat{c}_{33}	\hat{c}_{44}	\hat{c}_{66}
359	123	87	383	98	117	371	120	92	348	112	125

5. Piezoelectricity

We use the following constitutive equations

$$\hat{\sigma} = \hat{c}' : (\hat{\epsilon} - \hat{\epsilon}_{\text{ch}}) + \hat{e}^T \hat{\mathbf{E}}, \quad (24)$$

$$\hat{\mathbf{P}} = \hat{\epsilon} \hat{\mathbf{E}} + \hat{e} : (\hat{\epsilon} - \hat{\epsilon}_{\text{ch}}) + \hat{\mathbf{P}}_{\text{sp}}, \quad (25)$$

where the stiffness tensor satisfies the condition

$$\hat{c}' = \hat{c} + \hat{\mathbf{C}} : (\hat{\epsilon} - \hat{\epsilon}_{\text{ch}}), \quad (26)$$

$\hat{c}, \hat{\mathbf{C}}$ denote the second and third order elastic constants, and $\hat{e}, \hat{\epsilon}, \hat{\mathbf{P}}_{\text{sp}}$ are the piezoelectric, dielectric tensors and spontaneous polarization vector determined in relation to the undeformed configuration state. By assumption they all satisfy here a linear (Vegard) law dependent on $\frac{\text{Ga}}{\text{Ga+Al}}$ molar fraction, e.g.

$$\hat{\epsilon}_{\text{ch}} = \hat{\mathbf{a}}_{\text{GaN}} x + \hat{\mathbf{a}}_{\text{AlN}} (1 - x), \quad (27)$$

$$\hat{\mathbf{P}}_{\text{sp}} = \hat{\mathbf{P}}_{\text{spGaN}} x + \hat{\mathbf{P}}_{\text{spAlN}} (1 - x), \quad (28)$$

where $\hat{\mathbf{a}}_{\text{AlN}}$ and $\hat{\mathbf{a}}_{\text{GaN}}$ are the respective Vegard coefficients tensors.

6. Finite element method

We solve the following differential equation set

$$\begin{cases} \text{div } \boldsymbol{\sigma} = \mathbf{0}, \\ \text{div } \mathbf{P} = 0, \end{cases} \quad (29)$$

where the Cauchy stress and electric polarity referred to the current configuration are

$$\boldsymbol{\sigma} = \mathcal{A} : (\hat{\mathbf{c}} : (\hat{\epsilon} - \hat{\epsilon}_{\text{ch}}) + \hat{e}^T \hat{\mathbf{E}}) \det \mathbf{F}^{-1}, \quad (30)$$

$$\mathbf{P} = \mathbf{F} (\hat{\epsilon} \hat{\mathbf{E}} + \hat{e} : (\hat{\epsilon} - \hat{\epsilon}_{\text{ch}}) + \hat{\mathbf{P}}_{\text{sp}}) \det \mathbf{F}^{-1}. \quad (31)$$

The fourth order transformation tensor \mathcal{A} depends on strain, $\mathcal{A} = \mathcal{A}(\boldsymbol{\epsilon})$. The mathematical executive formula of the function $\mathcal{A}(\boldsymbol{\epsilon})$ transforming the stress conjugate by work with given strain measure to the Cauchy stress tensor depends on the choice of strain measure (see [5]). In FE simulations we have used the logarithmic (Hencky) strain for which the aforementioned formula rewritten in the strain eigenvector basis takes form

$$\hat{\mathcal{A}}_{ij} = \begin{cases} 1 & \text{for } \hat{\epsilon}_i = \hat{\epsilon}_j, \\ \frac{\hat{\epsilon}_i - \hat{\epsilon}_j}{\sinh(\hat{\epsilon}_i - \hat{\epsilon}_j)} & \text{for } \hat{\epsilon}_i \neq \hat{\epsilon}_j. \end{cases} \quad (32)$$

6.1. FE results

In the considered example we used 2616 3D brick second-order Lagrangian elements. The total size of the mesh was $10.925\text{nm} \times 10.925\text{nm} \times 12\text{nm}$. The QD is taken to have a truncated hexagonal pyramidal shape. The unit cell, along with the embedded QD are shown in Figure 1(a). The second and first order shape functions spanned respectively on 27 and 8-corner

nodes were employed. In each node the following 5 variables were stored: 3 nodal displacements, electric potential and $\frac{\text{Ga}}{\text{Ga+Al}}$ molar fraction. For molar fraction we used the first order (linear) 8-node shape function while to avoid elastic incompatibilities the second-order (parabolic) shape function was used both for the displacements and the electric potential. Thanks to this approach the chemical composition was obtained as a continuous multilinear function within finite elements as it is clearly depicted in Figure 1(b). The chemical composition was constrained in all nodes. In result, the boundary value problem was solved for not 5 but 4 degrees of freedom: 3 displacements + electric potential. The multipoint boundary condition was imposed on displacements in the z direction. The electric potential was assumed to be zero on the bottom and top surfaces.

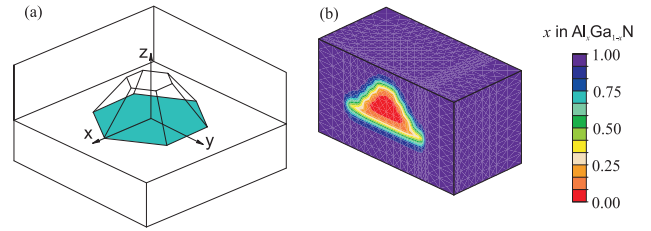


Figure 1: (a) Schematic representation of the simulation cell. The truncated pyramidal shape GaN QD is embedded in AlN host matrix. (b) Cross section cut of the simulation cell depicting the chemical composition distribution: The composition varies smoothly from $x = 0$ (pure AlN) in the host matrix to $x = 1$ (pure GaN) in the QD.

If Figure 2(a) and (b) the stress components σ_{xx} as derived from our FM calculations without and with using the third order elastic constants respectively are shown. Qualitative differences between the two distributions exists for the region at the top of the simulation cell above the QD. Quantitatively the use of third order elastic constants result in more than 6% larger absolute stress values. Similar effect was found for the other stress components.

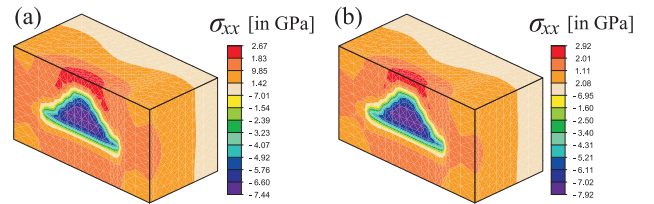


Figure 2: The stress components σ_{xx} calculated without (a) and with (b) taking into account the third order elastic constants.

In Figure 3(a) and (b) the electric potential distributions as derived from our FM calculations without and with using the third order elastic constants respectively are shown. Similar to the case of the stress components, both pictures are qualitatively similar. However, the use of third order elastic constants in the FEM calculations results in approximately 5% larger absolute values of the potential. This is nicely shown in Figure 4 where the potential along the z -axis for both cases is plotted ($x = y = 0$). As can be clearly seen there is a large difference of the potential between the bottom ($z = 0$ nm) and the top ($z = 4$ nm) of the QD of the order of ≈ 1.4 V with interesting consequences for the carriers localization: holes are expected to be attracted towards the negative values of the potential, namely towards the bottom of the

Table 2: Third order elastic constants [in GPa] determined by *ab-initio* calculations for the Biot strain measure. Based on the transformation rules for the subsystem 11 of the wurtzitic symmetry (Eqn 17), the values corresponding to the Green and Hencky strain measures are provided.

Strain measure	GaN										AlN									
	\hat{C}_{111}	\hat{C}_{222}	\hat{C}_{333}	\hat{C}_{112}	\hat{C}_{113}	\hat{C}_{123}	\hat{C}_{133}	\hat{C}_{144}	\hat{C}_{155}	\hat{C}_{344}	\hat{C}_{111}	\hat{C}_{222}	\hat{C}_{333}	\hat{C}_{112}	\hat{C}_{113}	\hat{C}_{123}	\hat{C}_{133}	\hat{C}_{144}	\hat{C}_{155}	\hat{C}_{344}
Biot	-1570	-1360	-1410	-580	-314	-461	-866	121	61	-5	-1830	-3000	187	-217	107	-315	-102	119	-375	-261
Green	-2740	-2530	-2664	-725	-420	-461	-972	58	-168	-236	-3064	-4226	-980	-366	8	-315	-1120	45	-640	-445
Hencky	-400	-190	-276	-435	-208	-461	-760	184	290	226	-604	-1766	1354	-68	206	-315	-921	194	-111	-77

QD, while on the other hand electrons are expected to be trapped towards the upper part of the QD. These results are in a good qualitative agreement with recent calculations by Williams *et al.* [17]: they also found a large deviation of the potential along the growth direction. However, differences in the profile of the potential distribution as well as in the absolute values of the potential may be well attributed to a number of different assumption taken in both works. For example in Ref. [17] it is assumed that the system is electromechanically uncoupled, and the same isotropic elastic constants are assumed for both the dot (GaN) and the host matrix (AlN) materials.

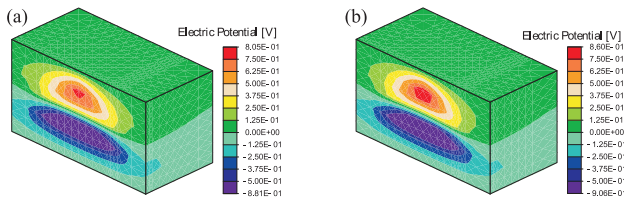


Figure 3: The electric potential distributions calculated without (a) and with (b) taking into account the third order elastic constants.

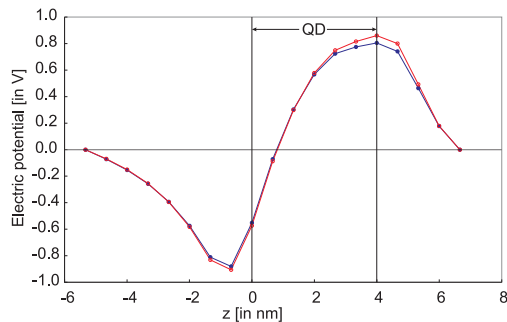


Figure 4: Electric potential along the z -axis ($x = y = 0$) calculated with (blue line) and without (red line) taking into account the non-linear effects on the elastic constants. The GaN QD is embedded in the region from $z=0$ to $z=4$ nm. The boundary conditions used assume the potential to vanish at the top and the bottom of the simulation cell.

7. Conclusions

In this paper we have combined *ab-initio* calculations of the second and third order elastic constants with FEM calculations of the strain and polarization constitutive equations, in order to study the system of a truncated pyramidal shape GaN QD embedded in an AlN host matrix. The 10 independent third order

elastic constants associated with the wurtzitic crystal symmetry have been determined by applying corresponding strain deformations along six linearly independent strain directions. The advantage of this approach is that it provides the strain measure independent elastic constants. It has been shown that the third order elastic constants depend sensitively on the strain measure (see Table 1). However, it is worth emphasizing that the so-called linear strain measure called also infinitesimal strain measure does not determine the deformed configuration, uniquely. In result, any comparison and/or quantitative analysis of the third order elastic constants determined with the use of the linear strain measure is impossible. Our calculations also reveal that the Vegard's law is an excellent approximation for the second order elastic constants of AlGaN alloys.

The electric potential distribution within the QD is of great importance for the spatial localization of the carriers. We have shown that the electric field varies significantly along the growth direction: It is negative at the bottom of the QD while it takes positive values at the top of the QD. Thus it is expected that holes will be attracted at the bottom while electrons at the top of the nanostructure. Finally, we have shown that the inclusion of third order elastic constants in our FEM calculation does not qualitatively change the potential distribution associated with the QD system. However, we have also shown that non-linear effects result in up to 5% larger absolute electric potential values. It is under question if this change may significantly influence the energy states and the spatial localization of the carriers. It is a matter of further $k \cdot p$ calculations which will integrate into the Hamiltonian the stress, and potential distributions derived from the FEM calculations, in order to investigate the of non-linearity on the QD electron and holes states.

8. Acknowledgment

This work is supported by EU Marie Curie RTN contract MRTN-CT-2004-005583 (PARSEM) and grant 131/6PRUE/2005/7 founded by the Polish Ministry of Science and Higher Education.

References

- [1] *Properties, Processing and Applications of Gallium Nitride and Related Materials*, volume 23 of EMIS Datareview Series. INSPEC, London, 1999.
- [2] F. Bechstedt and J. Furthmüller. Do we know the fundamental energy gap of inn? *Journal of Crystal Growth*, 246:315–319, 2002.
- [3] K. Brugger. Thermodynamic definition of higher order elastic coefficients. *Physical Review*, 133(6A):1611–12, 1964.
- [4] Z. Curnier and Ph. Zysset. A family of metric strains and conjugate stresses, prolonging usual material laws from small to large transformations. *International Journal of*

Solids and Structures, 43:3057–3086, 2006.

- [5] P. Dłużewski. Anisotropic hyperelasticity based upon general strain measures. *Journal of Elasticity*, 60(2):119–129, 2000.
- [6] Y. Hiki and A. V. Granato. Anharmonicity in noble metals; higher order elastic constants. *Physical Review*, 144(2):411–19, 1966.
- [7] R. Hill. Constitutive inequalities for isotropic solids under finite strain. *Proceedings of Royal Society of London A*, 314:457–472, 1970.
- [8] <http://www.sfhingx.de>.
- [9] S.P. Łepkowski, J. Majewski, and G. Jurczak. Nonlinear elasticity in III-N compounds: Ab initio calculations. *Physical Review B*, 73:245201, 2005.
- [10] R. W. Ogden. *Non-Linear Elastic Deformations*. Ellis Horwood Ltd., Chichester, 1984.
- [11] P. Rinke, M. Scheffler, A. Qteish, M. Winkelkemper, D. Bimberg, and J. Neugebauer. Band gap and band parameters of InN and GaN from quasiparticle energy calculations based on exact-exchange density-functional theory. *Applied Physics Letters*, 89:161919, 2006.
- [12] B. R. Seth. Generalized strain measure with applications to physical problems. In M. Reiner and D. Abir, editors, *Second-Order Effects in Elasticity, Plasticity and Fluid Dynamics, Proceedings of International Symposium, Haifa, April 23-27, 1962*, pages 162–172, Oxford, 1964. Pergamon Press.
- [13] S. Sutcliffe. Spectral decomposition of the elasticity tensor. *ASME Journal of Applied Mechanics*, 59(4):762–773, 1992.
- [14] R. N. Thurston and K. Brugger. Third-order elastic constants and the velocity of small amplitude elastic waves in homogeneously stressed media. *Physical Review*, 133(6A):1604–1610, 1964.
- [15] N. Troullier and J. L. Martins. Efficient pseudopotentials for plane-wave calculations. *Physical Review B*, 43(1993), 1991.
- [16] N. J. Walker, G. A. Saunders, and J. E. Hawkey. Soft TA models and anharmonicity in cadmium telluride. *Physical Review B*, 52(5):1005–1018, 1985.
- [17] D. P. Williams, A. D. Andreev, E. P. O’Reilly, and D. A. Faux. Derivation of built-in polarization potentials in nitride-based semiconductor quantum dots. *Physical Review B*, 72:235318, 2005.
- [18] A. Zunger, S.H. Wei, L.G. Ferreira, and J.E. Bernard. Special quasirandom structures. *Physical Review Letters*, 65(353), 1991.